

Decay Scheme of  $\text{Br}^{82}\dagger$ 

R. C. WADDELL\* AND E. N. JENSEN

*Institute for Atomic Research and Department of Physics, Iowa State College, Ames, Iowa*

(Received January 25, 1956)

The radiations from  $\text{Br}^{82}$  were studied using an intermediate-image coincidence spectrometer, gamma-gamma coincidence scintillation spectrometer, and gamma-gamma directional correlation equipment. One allowed beta-ray group and eight gamma rays were observed. An energy level diagram is proposed. Determinations of the energies, relative intensities, and internal conversion coefficients were made. Five directional correlation measurements were performed between various gamma-ray combinations. Unambiguous assignments for the spins and parities of four of the first five excited levels are made, while the assignment for the remaining level is restricted to two possible values. Multipole mixing ratios were measured for three of the transitions. A possible interpretation of the excited states, in terms of vibrational levels, is proposed.

## I. INTRODUCTION

THE radiations from  $\text{Br}^{82}$  have been examined by several groups employing magnetic spectrometers,<sup>1-5</sup> but no coincidence techniques were used. A total of eight gamma-ray energies were reported, with additional higher energy radiations possible. An intense beta group was found with the possibility that very weak lower energy beta groups could exist. A study of the gamma rays from  $\text{Br}^{82}$ , using scintillation summing techniques, was made by Lu *et al.*<sup>6</sup> They proposed an energy level diagram.

Magnetic spectrometer measurements of the radiations from the 6.3-hour  $\text{Rb}^{82}$  have been made by two groups.<sup>7, 8</sup> No coincidence work was done. All of the gamma rays found in the decay of  $\text{Br}^{82}$  were observed in the decay of  $\text{Rb}^{82}$  and in addition several of lower energy were reported. Energy level diagrams were proposed.

In the investigation reported in this paper, coincidence and direct measurements were made using an intermediate-image spectrometer<sup>9</sup> and a conventional gamma-gamma coincidence scintillation spectrometer. Directional correlation measurements were made between gamma rays selected by pulse height analysis. From these data it was possible to construct a decay scheme in which spins and parities were assigned as well as relative gamma-ray intensities. In three cases multipole mixtures were determined.

## II. EXPERIMENTAL PROCEDURE

A source for use in the intermediate-image spectrometer was prepared by evaporating the water from two drops of a  $\text{MgBr}_2$  solution placed on an aluminized collodion film. The average density of source and backing was less than 1 mg/cm<sup>2</sup>. Use of the formula of Hamilton and Gross<sup>10</sup> gives estimates that scattering effects should become significant at energies of about 180 kev, which is well below that of the lowest energy conversion line. Measurements were delayed for approximately 100 hours after removing the activated  $\text{MgBr}^2$  from the CP-5 pile at Argonne National Laboratory thus allowing the 4.6-hour  $\text{Br}^{80m}$  activity to decay out.

The beta spectrum and internal conversion lines were obtained with the resolution of the intermediate-image spectrometer set to 3%. Coincidence measurements, with the intermediate-image spectrometer, were made by setting the associated gamma-ray scintillation spectrometer on the high-energy gamma rays and sweeping the magnetic spectrometer over the region of interest. This procedure was repeated to obtain those conversion electrons in coincidence with lower energy gamma rays. For the coincidence measurements, the resolution of the intermediate-image spectrometer was set to 6%.

The scintillation spectrometer was used to obtain a single-channel gamma-ray spectrum of  $\text{Br}^{82}$ . The high-energy region was examined carefully with an intense source located at a distance of 15 feet from the detector, as well as at its usual distance of two inches.

The relative efficiency, for detection under the photopeaks by the scintillation spectrometer, was determined by measurements of the gamma-ray spectrum of  $\text{Bi}^{207}$ , whose gamma-ray intensities are well known.<sup>11</sup>

Coincidence measurements were made, using the coincidence scintillation spectrometer, by setting on the highest energy (1.47-Mev) gamma ray with the window of one pulse-height analyzer and sweeping the spectrum with the window of the other. This procedure was then repeated for the lower energy radiations.

<sup>†</sup> Contribution No. 429. Work was performed in the Ames Laboratory of the U. S. Atomic Energy Commission.

\* Now at Eastern Illinois State College, Charleston, Illinois.

<sup>1</sup> Roberts, Downing, and Deutsch, Phys. Rev. **60**, 544 (1941).

<sup>2</sup> Siegbahn, Hedgran, and Deutsch, Phys. Rev. **76**, 1263 (1949).

<sup>3</sup> V. Meyers and A. Wattenberg, Phys. Rev. **75**, 992 (1949).

<sup>4</sup> P. Hubert and J. Laberrie-Frolow, Compt. rend. **232**, 2420 (1951).

<sup>5</sup> B. Dzhelepov and A. Stlant'ev, Doklady Akad. Nauk S.S.S.R. **85**, 533 (1952).

<sup>6</sup> Lu, Kelly, and Wiedenbeck, Phys. Rev. **95**, 1533 (1954).

<sup>7</sup> C. M. Huddleston and A. C. G. Mitchell, Phys. Rev. **88**, 1350 (1952).

<sup>8</sup> H. T. Easterday, University of California Radiation Laboratory Report UCRL-2172, 1953 (unpublished).

<sup>9</sup> Nichols, Pohn, Talboy, and Jensen, Rev. Sci. Instr. **26**, 580 (1955).

<sup>10</sup> D. R. Hamilton and L. Gross, Rev. Sci. Instr. **21**, 912 (1950).

<sup>11</sup> D. E. Alburger and A. W. Sunyar, Phys. Rev. **99**, 695 (1955).

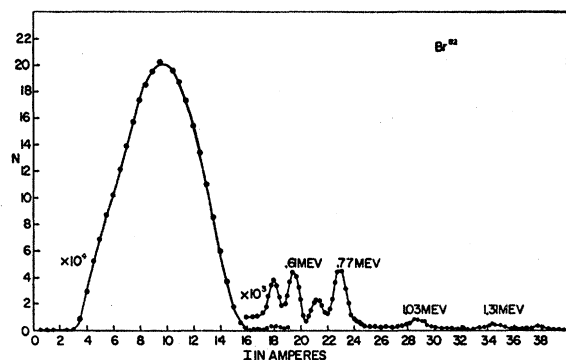


FIG. 1. Beta and internal conversion spectrum obtained with the intermediate-image spectrometer set for 3% resolution.  $N$  is the counting rate.

The coincidence scintillation spectrometer was used in the directional correlation measurements by setting the detectors in the horizontal plane containing the source. Provisions existed for accurately centering the source and moving one detector arm in integral increments of  $15^\circ$  from  $90^\circ$  relative to the fixed detector through  $270^\circ$ . No lead shielding was used, as separation of gamma rays was accomplished entirely by pulse-height analysis.

Corrections for the finite geometry subtended by the detectors were made using the method of Lawson and Frauenfelder.<sup>12</sup> The gamma rays of  $\text{Co}^{60}$  and  $\text{Cs}^{137}$  were used in making the geometrical corrections for  $\text{Br}^{82}$  directional correlations involving high- and low-energy radiations.

No corrections were made for finite source size in the directional correlation work. Sources were generally in the form of  $\text{NaBr}$  in a dilute water solution except in the one measurement in which the effect of source state was considered. Liquid and dry  $\text{MgBr}_2$  was used for this work. To average out fluctuations, data were taken in cyclic fashion with the time at each of the 14 angular positions limited to 10 minutes.

Corrections for the accidental coincidences were made

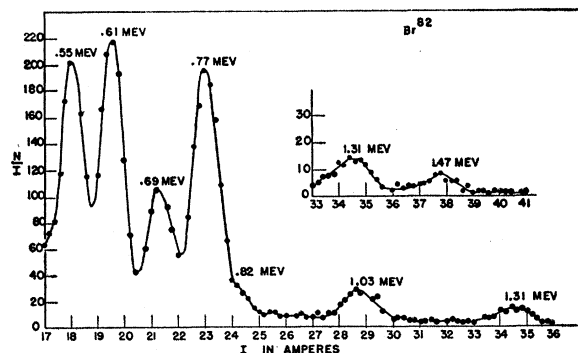


FIG. 2.  $N/I$  plot of the internal conversion spectrum from which the gamma-ray energies and relative conversion intensities were obtained.  $N$  is the counting rate.

<sup>12</sup> J. S. Lawson and H. Frauenfelder, Phys. Rev. **91**, 649 (1953).

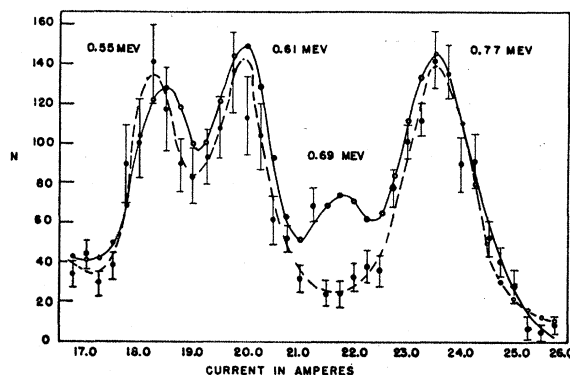


FIG. 3. The solid curve represents the conversion spectrum while the dashed curve shows the conversion electrons in coincidence with the 1.03-, 1.30-, and 1.47-Mev gamma rays.  $N$  is the counting rate.

by calculating the number of accidentals using the known single-channel rates and the coincidence resolving time. The resolving time was measured often during correlation measurements and was found to be constant over long periods of time. For most of the measurements the value of the resolving time was about  $5 \times 10^{-7}$  sec.

The known directional distribution of  $\text{Co}^{60}$  was measured as a check on the performance of the directional correlation equipment. An anisotropy of  $0.169 \pm 0.005$  was obtained.

### III. EXPERIMENTAL RESULTS

The beta and internal conversion spectrum is shown in Fig. 1, while Fig. 2 displays, in an  $N/I$  plot, the internal conversion region of the spectrum. Energies of the gamma rays and relative intensities of the conversion lines, obtained from the  $N/I$  plot, are given in Table I. The end-point energy, obtained from the linear Kurie plot of the single beta group observed in this work, is  $444 \pm 1$  kev. The  $\log ft$  value is 5.1, indicating an allowed  $\beta$  transition. Figure 3 displays the coincidence conversion spectrum, as observed with the

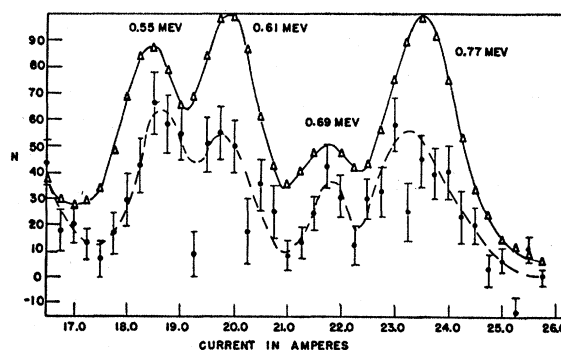


FIG. 4. The solid curve represents the conversion spectrum while the dashed curve shows the conversion electrons in coincidence with all gamma rays above 0.70 Mev.  $N$  is the counting rate.

TABLE I. Transition energies, relative intensities, and conversion coefficients of  $\text{Br}^{82}$  radiations.

Energy (Mev)	0.545 $\pm$ 0.002	0.610 $\pm$ 0.002	0.688 $\pm$ 0.002	0.766 $\pm$ 0.003	0.817 $\pm$ 0.007	1.029 $\pm$ 0.005	1.305 $\pm$ 0.005	1.469 $\pm$ 0.007
Rel. conv. intensity	0.87 $\pm$ 10%	1.0 $\pm$ 5%	0.51 $\pm$ 5%	1.0 $\pm$ 10%	0.12 $\pm$ 20%	0.16 $\pm$ 5%	0.08 $\pm$ 5%	0.04 $\pm$ 10%
Rel. gamma intensity	1.02 $\pm$ 10%	0.50 $\pm$ 10%	0.37 $\pm$ 15%	1.0 $\pm$ 10%	0.30 $\pm$ 20%	0.36 $\pm$ 5%	0.36 $\pm$ 10%	0.18 $\pm$ 15%
Measured int. conv. coefficient $\times 10^3$	0.68 $\pm$ 14%	1.60 $\pm$ 11%	1.1 $\pm$ 15%	1.00 $\pm$ 20%	0.32 $\pm$ 30%	0.36 $\pm$ 10%	0.18 $\pm$ 11%	0.18 $\pm$ 18%
Theoretical conv. coefficient $\times 10^3$	E1, 0.68	E2, 1.6	E2, 1.1	E2, 0.08	E1, 0.27	M1, E2, 0.39	M1, E2, 0.22	M1, E2, 0.19
Rose <i>et al.</i> <sup>a</sup>	M1, 1.4	M1, 1.2	M1, 0.9		M1, 0.60	M2, E3, 0.80	M2, E3, 0.45	E3, M2, 0.33

<sup>a</sup> Rose, Goertzel, and Perry, Oak Ridge National Laboratory Report ORNL 1023, 1951 (unpublished).

intermediate-image spectrometer, with the associated gamma-ray analyzer set integrally to pass the photopeak of the 1.03-Mev gamma ray and the pulses from the 1.30- and 1.47-Mev gamma rays which are above the 1.03-Mev photopeak. Figure 3 indicates that one or more of the 1.03-, 1.30-, and 1.47-Mev gamma rays are in coincidence with one or more of the 0.55-, 0.61-, and 0.77-Mev gamma rays and that none of the 1.03-, 1.30-, and 1.47-Mev radiations are in coincidence with the 0.69-Mev gamma ray. Figure 4 shows the same region with the analyzer set to window on the photopeak of the 0.77-Mev gamma ray. One notes that the 0.69-Mev conversion line is well resolved in this work. Figure 4 indicates that the 0.77-Mev gamma ray is in coincidence with the 0.69-Mev gamma ray. An addi-

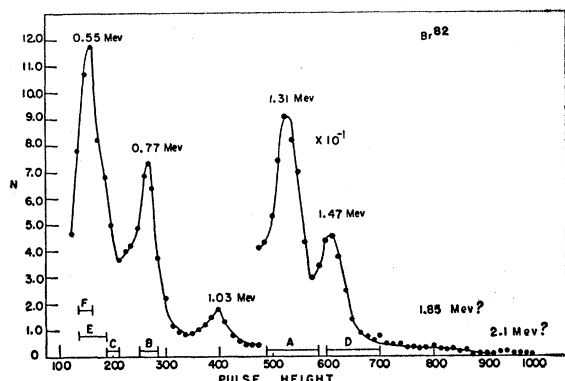


FIG. 5. Scintillation spectrum of  $\text{Br}^{82}$ . The lettered regions correspond to window settings described in text.

tional measurement, with the gamma-ray analyzer set to pass the photopeaks of the 1.30- and 1.47-Mev gamma rays, gave essentially the same result as shown in Fig. 3.

Figure 5 shows the single-channel scintillation spectrum of  $\text{Br}^{82}$ . One notes small peaks in the region above 700 pulse height units. These essentially disappear upon moving the source 15 ft back from the detector, indicating they are predominately sum lines. However, weak high-energy radiations may exist. In order to estimate the relative intensities of the gamma rays, a procedure, similar to that described by McGowan,<sup>13</sup> was used to remove the effects of Compton-scattered radiation. Figure 6 shows the low-energy region of the scintillation spectrum with the estimated layers of

<sup>13</sup> F. K. McGowan, Phys. Rev. 93, 163 (1954).

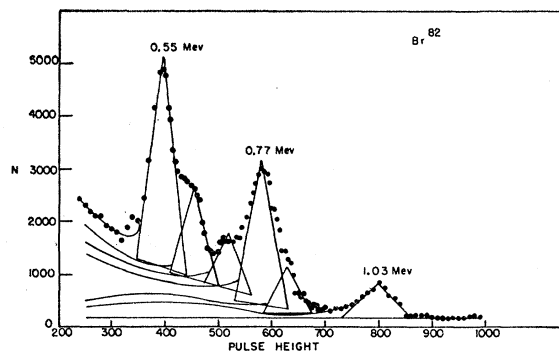


FIG. 6. Expanded low-energy region of the  $\text{Br}^{82}$  scintillation spectrum. The additional lines show the synthesized Compton distributions and triangles used to approximate the photopeaks used in estimating relative intensities.

Compton radiation. Triangles were used to approximate the actual photopeaks in obtaining relative intensities. Table I gives the relative gamma-ray intensities obtained by this procedure.

Figure 7, obtained by using the gamma-gamma scintillation coincidence spectrometer and windowing on the 1.47-Mev photopeak, indicates that the 1.47-Mev gamma ray is in coincidence with both the 0.55-

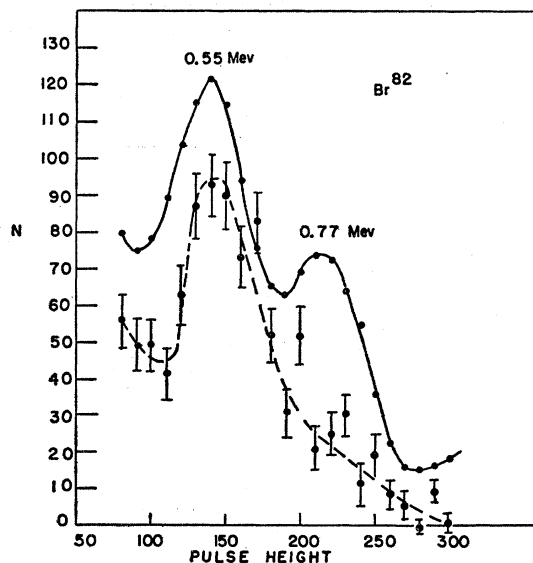


FIG. 7. The dashed curve shows radiation in coincidence with 1.47-Mev gamma ray. The solid curve is  $\text{Br}^{82}$  single-channel scintillation spectrum.

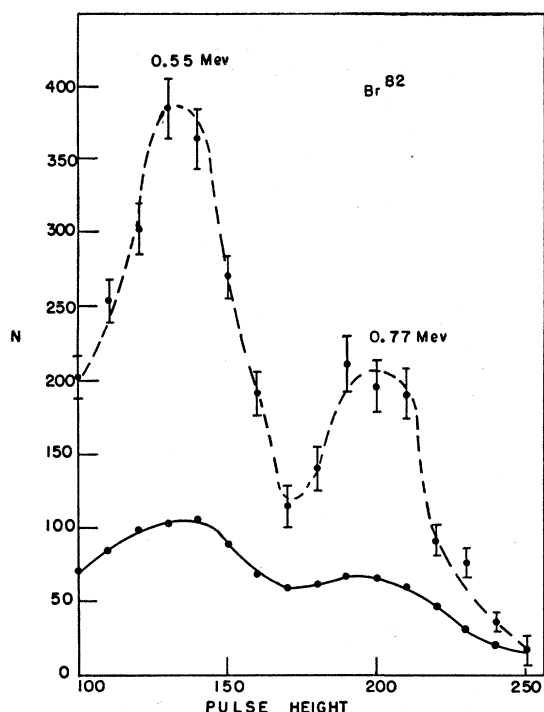


FIG. 8. The dashed curve shows gamma rays in coincidence with 1.30-Mev gamma ray and Compton-scattered radiation from the 1.47-Mev radiation. The solid curve is the  $\text{Br}^{82}$  single-channel spectrum.

and 0.61-Mev radiations, but is not in coincidence with the 0.77-Mev gamma ray. Figure 8, obtained by windowing on the photopeak of the 1.30-Mev gamma ray (but also passing Compton-scattered radiation from the 1.47-Mev gamma ray) indicates that the 0.77-Mev gamma ray is in coincidence with the 1.30-Mev radiation.

A consideration of the energies of the transitions, along with the coincidence results, permits the presentation of the decay scheme shown in Fig. 9. This diagram is an inversion of the one proposed by Lu *et al.*<sup>6</sup> Two arguments can be advanced to prove the inversion is necessary. (1) The 0.77-Mev gamma ray, from the decay of  $\text{Rb}^{82}$ , has been shown<sup>7,8</sup> to be the most intense. It should thus be to the ground state. (2) The ground-state radiation from the first excited state of an even-even nucleus is expected to be pure  $E2$ . As will be shown later, the internal conversion coefficient of the 0.77-Mev transition indicates it to be  $E2$ , while that of the 0.55-Mev transition indicates it to be  $E1$ .

The internal conversion coefficient of the 0.77-Mev transition was obtained by a direct comparison of the areas, obtained from an  $N/I$  plot, under the beta spectrum and the conversion line. The relative intensity of the 1.47-Mev radiation, which is parallel to the 0.77-Mev radiation, was considered. All of the conversion lines observed were assumed to be from the  $K$ -shell as measurements, using 1% resolution,<sup>2</sup> did not detect  $L$ -shell electrons. After ascertaining directly

that the 0.77-Mev internal conversion coefficient indicated an  $E2$  transition and that the 0.55-Mev transition could not be  $E2$ , the coefficients of all but the 0.77-Mev transition were obtained by comparing relative conversion and gamma-ray intensities and using the proportionality constant obtained from the known 0.77-Mev  $E2$  transition. The conversion coefficients are given in Table I.

Two measurements of the directional distribution function between the 0.77- and 1.30-Mev gamma rays were made. The analyzer windows were set as indicated by letters *A* and *B* of Fig. 5. Figure 10 shows the experimental results, which have not been corrected for detector geometry, for the directional correlation  $C(\theta)$ . For one run the value of the mean square residual  $\epsilon^2$ , in the notation of Rose,<sup>14</sup> is 3.2 while for the other this value is 0.90. A value of  $\epsilon^2$  around unity indicates that certain systematic errors are not present. The weighted mean values of the coefficients  $A_2$  and  $A_4$  in the equation  $W(\theta) = 1 + A_2 P_2(\cos\theta) + A_4 P_4(\cos\theta)$ , for the 0.77- and 1.30-Mev directional distribution, corrected for detector geometry, are given in Table II as correlation number (1). A consideration of the geometry, relative intensities, and relative detector efficiencies showed that the contribution to the given distribution function, of the unknown triple correlation resulting from summing of the 0.69- and 0.61-Mev radiations, was about

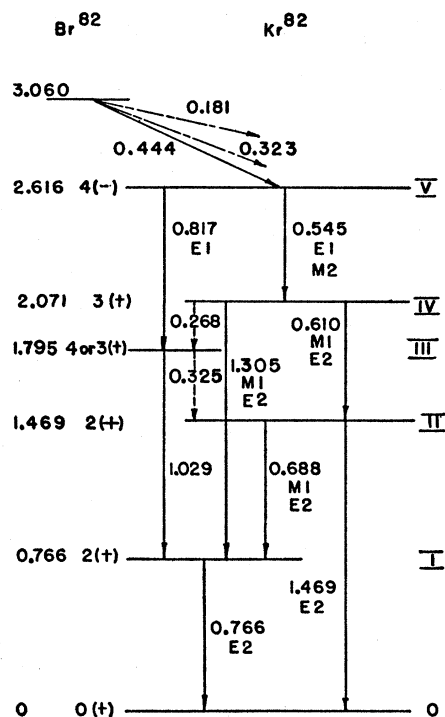


FIG. 9. Proposed energy (Mev) level diagram. Radiations represented by dashed lines were reported by Easterday<sup>8</sup> and Huddleston and Mitchell.<sup>7</sup>

<sup>14</sup> M. E. Rose, Phys. Rev. **91**, 610 (1953).

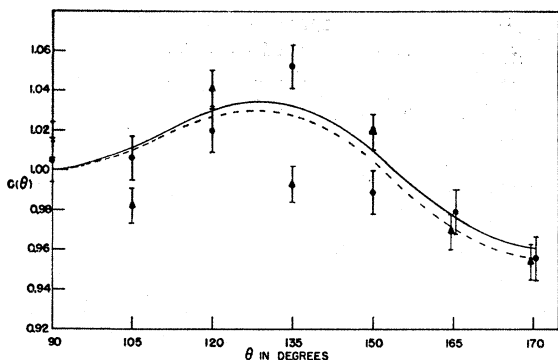


FIG. 10. The dashed curve represents the least squares fit of the 1.30-0.77 Mev cascade. The solid curve shows the  $3(D+Q)2(Q)0$  transition. For the run ●, the mean square residual  $\epsilon^2=0.90$ , while the run ▲ corresponds to  $\epsilon^2=3.2$ .

one percent. To ascertain that this amount was insignificant, the correlation was obtained a third time with the 1.30-Mev gamma-ray detector to source distance doubled. The distribution was essentially unchanged.

Two measurements of the 0.61-1.47 Mev cascade were made with the analyzer windows set as indicated by the letters *C* and *D* of Fig. 5. The experimental results are indicated in Fig. 11. The weighted mean values of the coefficients, corrected for detector geometry, are given in Table II as correlation number (2).

A single measurement of the 0.55-0.61 Mev cascade was made with the windows set as indicated by letter *E* of Fig. 5. Figure 12 shows the experimental results. The coefficient of the distribution is given in Table II as correlation number (5). A small percentage of unknown interfering distributions is contained in the listed value.

The results of two measurements of the 0.55-1.30 Mev cascade, with the windows set as indicated by letters *F* and *A* of Fig. 5, are shown in Fig. 13. One notes that the values of  $\epsilon^2$  are 0.17 and 5. An estimate of the effect of the interfering (0.55+0.61)-1.47 Mev and 0.77-1.30 Mev distributions was made and subtracted to give the coefficient listed in Table II as correlation number (4).

The triple correlation, with the intermediate radiation unobserved, between the 0.55- and 1.47-Mev gamma rays, was measured twice. The values of  $\epsilon^2$  obtained

TABLE II. Experimentally obtained coefficients of the distribution  $W(\theta)=1+A_2P_2(\cos\theta)+A_4P_4(\cos\theta)$ .

Gamma-ray energies in Mev	Correlation number	$A_2$	$A_4$
0.77-1.30	(1)	$-0.011 \pm 0.008$	$-0.074 \pm 0.013$
0.61-1.47	(2)	$+0.106 \pm 0.003$	$-0.052 \pm 0.010$
0.55-1.47 <sup>a</sup>	(3)	$-0.039 \pm 0.008$	
0.55-1.30 <sup>a</sup>	(4)	$-0.08 \pm 0.03$	$+0.01 \pm 0.01$
0.55-0.61 <sup>b</sup>	(5)	$-0.046 \pm 0.005$	

<sup>a</sup> Obtained by subtraction.

<sup>b</sup> Contains interfering distributions.

were 4.3 and 0.33. Upon subtracting the interfering 0.61-1.47 Mev radiation and correcting for detector geometry the coefficient listed in Table II was obtained as correlation number (3).

The anisotropy of the 0.55-0.61 Mev cascade was measured two times. For the first determination the source was a dilute water solution of  $MgBr_2$ , while for the second the same source had been evaporated to dryness under a heat lamp. No change outside of statistics, was observed.

#### IV. INTERPRETATION OF EXPERIMENTAL RESULTS

Assume the ground state of even-even  $Kr^{82}$  to have zero units of angular momentum and even parity, designated by  $0(+)$ . The measured internal conversion coefficient of the 0.77-Mev transition (see Table I) indicates that it is *E2*, hence the first excited state, i.e., level I, is  $2(+)$ . (See Fig. 9.)

The measured internal conversion coefficient of the 1.47-Mev transition can be interpreted as *M1*, *E2*, *M2*, or *E3*. As correlation (2) of Table II has a nonzero  $A_4$ , a spin of one unit can be eliminated from consideration for level II. Level II could thus be  $2(+)$ ,  $2(-)$ , or  $3(-)$ . The measured internal conversion coefficient of the 0.69-Mev radiation can be interpreted as either *M1* or *E2*. This restricts level II to a spin of 1, 2, 3, or 4 with even parity. Hence level II must be  $2(+)$ . This assignment is not inconsistent with the relative intensities of the 0.69- and 1.47-Mev radiations, predicted by the single particle model, as obtained from the monogram of Montalbetti.<sup>15</sup>

The measured internal conversion coefficient of the 1.30-Mev transition indicates that it is either *M1* or *E2*. Level IV is restricted to a spin of 0, 1, 2, 3, or 4, with even parity. The internal conversion coefficient of the 0.61-Mev radiation is consistent with these assignments. Correlation distributions (1) and (2) of Table II eliminate the possibility of pure radiations from any of these possibilities. Consider a mixture of dipole (*D*)

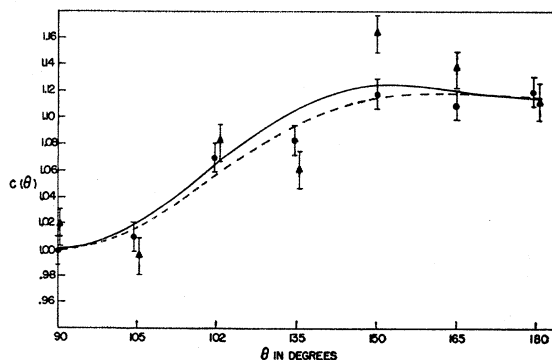


FIG. 11. The dashed curve represents the least squares fit of the 1.47-0.61 Mev cascade. The solid curve represents the  $3(D+Q)2(Q)0$  transition. The run ● corresponds to a mean square residual  $\epsilon^2=0.4$  while the run ▲ corresponds to  $\epsilon^2=2.6$ .

<sup>15</sup> R. Montalbetti, Can. J. Phys. 30, 660 (1952).

and quadrupole ( $Q$ ) components in the 1.30- and 0.61-Mev gamma radiations from level IV with an assumed spin of either 2 or 4. One finds that  $\delta$ , the ratio of the  $Q$  to  $D$  matrix elements, is imaginary for a transition between these levels if  $A_4 < 0$ . Lloyd<sup>16</sup> states that  $\delta$  may be either positive or negative but must be real. Hence level IV cannot be either 2(+) or 4(+). As correlations (3), (4), and (5) of Table II are not isotropic, level IV cannot be 0(+). Consider the possibility of level IV being 1(+). As an  $A_4$  term exists in both correlations (1) and (2), the 1.30-Mev and 0.61-Mev radiations must each be a mixture of  $D$  and  $Q$  components. In order to evaluate  $\delta$  one can plot curves of the theoretically predicted coefficients  $A_2$  and  $A_4$  as a function of  $|\delta|$  or of  $\log |\delta|$ . As  $\delta$  may be either positive or negative, two solutions of the  $A_2$  equation exist, corresponding to the two values  $\delta \gtrless 0$ , while for the  $A_4$  equation, as  $\delta$  enters only in the square, a single solution exists. Figure 14 shows the solutions of the  $A_2$  and  $A_4$  equations

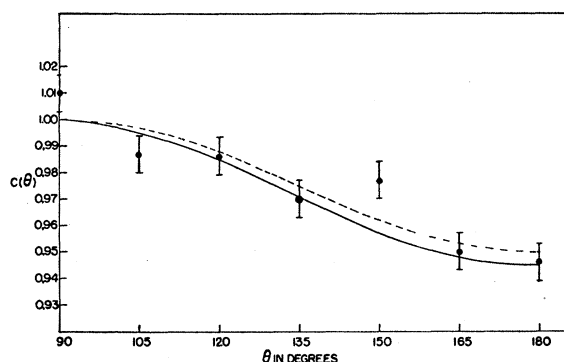


FIG. 12. The dashed curve represents the least squares fit to the indicated experimental points. The solid curve represents the  $4(D+Q)3(D+Q)2$  cascade of the 0.55–0.61 Mev radiations.

for the  $1(D+Q)2(Q)0$  cascade, along with the experimentally determined coefficients of both the 1.30–0.77 Mev and 0.61–1.47 Mev correlations. For the latter cascade, the value of  $\delta$ , consistent with both the  $A_2$  and  $A_4$  conditions, is  $\delta = +0.289$ .

In order to determine if the assignment of spin one to level IV is consistent with other experimental evidence, one must consider possibilities for level V. The internal conversion coefficient for the 0.55-Mev transition allows only an  $E1$  assignment. If level IV is 1(+), then level V must have a spin of 0, 1, or 2, with odd parity. If level V had a spin of either 1 or 2, intense radiations should go to levels 0, I, and II. These are not observed. If level IV has a spin of one then level V must have a spin of zero. Selection rules would allow a pure  $E1$  0.55-Mev transition only. As the  $\delta$  of the 0.61-Mev radiation has been found to be 0.289, the theoretical distribution function of the 0.55- and 0.61-Mev cascade was found to be  $W(\theta) = 1 + 0.325P_2(\cos\theta)$ ,

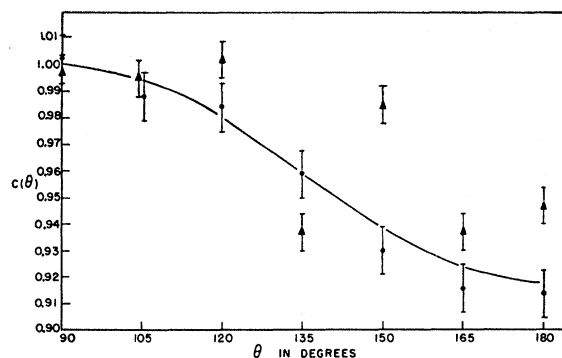


FIG. 13. The curve represents least squares fit to data obtained in 0.55–1.30 Mev correlation. The run ● indicates measurements with  $\epsilon^2 = 0.17$  while the run ▲ had  $\epsilon^2 = 5$ .

which is at variance with the experimentally determined correlation function (5) of Table II. Hence the possibility of 1(+) for level IV must be discarded. This rejection is consistent with the lack of a ground state transition, predicted by the single particle model, for this assignment.

Consider the remaining possibility of level IV being 3(+) with the radiations from that level being a  $D+Q$  mixture. Figure 15 shows the coefficients as a function of  $\log |\delta|$  for a  $3(D+Q)2(Q)0$  cascade. The experimentally obtained coefficients for both the 0.77–1.30 Mev and 0.61–1.47 Mev cascades are shown.

The value of  $\delta$  obtained from Fig. 15 for the 0.77–1.30 Mev cascade is  $-3.975$ . Thus the  $E2$  intensity of the 1.30-Mev transition is 15.8 times that of the  $M1$  component. The directional distribution, corrected for detector geometry, obtained using this value of  $\delta$  is also shown on Fig. 10.

The value of  $\delta$  for the 0.61–1.47 Mev cascade was found to be  $-2.3$ . The quadrupole component of the 0.61-Mev transition is thus 5.29 times the intensity of the dipole component. The distribution, corrected for detector geometry, for this  $\delta$  is shown in Fig. 11.

The assignment of 3(+) to level IV is the only

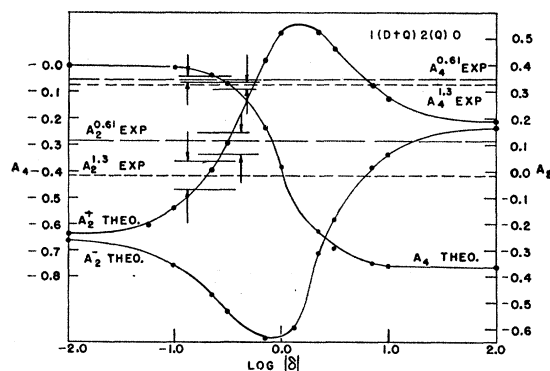


FIG. 14. Coefficients  $A_2^+$  and  $A_2^-$ , for  $\delta > 0$  and  $\delta < 0$ , respectively, and  $A_4$  as a function of  $\log |\delta|$ . Experimental values are as designated.

<sup>16</sup> S. P. Lloyd, Phys. Rev. **81**, 161 (1951).

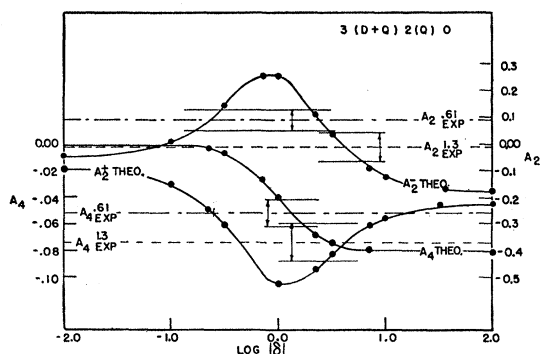


FIG. 15. Coefficients  $A_2^+$  and  $A_2^-$ , for  $\delta > 0$  and  $\delta < 0$ , respectively, and  $A_4$  as a function of  $\log|\delta|$ . Experimental values are as designated.

possible one that does not contradict the experimental evidence.

The internal conversion coefficient of the 0.55-Mev transition can only be interpreted as  $E1$ . This limits level V to a spin of 2, 3, or 4, with odd parity. The absence of transitions to levels 0, I, and II eliminate the first two of these possibilities. Assume level V to be 4(-). Correlation (5) of Table II precludes the possibility of the 0.55-Mev radiation being pure  $E1$ . Assume a multipole mixture of  $D$  and  $Q$  with a value  $\delta_0$ . As the mixing ratio for the 0.61-Mev transition has been determined, it is possible, using the theory of mixed-mixed transition,<sup>17</sup> to plot the coefficients  $A_2$  and  $A_4$  as a function of  $\log|\delta_0|$  as shown in Fig. 16. The value of  $\delta_0$  obtained from this figure is  $-0.1539$ , indicating that the  $M2$  intensity is 2.37 percent of the  $E1$  component of the 0.55-Mev radiation. The predicted distribution, corrected for detector geometry, for a  $4(D+Q)3(D+Q)2$  cascade with the above mixtures, is also shown on Fig. 12. Level V, therefore, appears to be 4(-).

Cross checks on the assignments made above consisted of comparing the observed 0.55–1.30 Mev and the 0.55–1.47 Mev directional distributions with those predicted using the assigned spins and mixtures. Reasonable agreement existed. Rose<sup>18</sup> has developed the theory of mixed triple cascades with the intermediate radiation unobserved.

The ordering of the 0.82–1.03 Mev cascade is uncertain. However, intensity considerations favor the order shown in Fig. 9. The internal conversion coefficient of the 0.82-Mev radiation indicates that it is  $E1$ , while that of the 1.03-Mev radiation is either  $M1$  or  $E2$ . These values require that level III be either 3(+) or 4(+). The intensities of the observed radiations are consistent with either of these possibilities. If the ordering were inverted, level III would need be either 2(-) or 3(-). Low energy radiations, observed in the

decay of  $\text{Rb}^{82}$ ,<sup>7,8</sup> can be fitted into the decay scheme with the order shown in Fig. 9.

If one assumes that the allowed 0.77-Mev positron group of the 6.3-hour  $\text{Rb}^{82}$  decays to level V as indicated by Way *et al.*,<sup>19</sup> 5(-) is the highest spin assignment that can be made for the  $\text{Rb}^{82m}$ .

## V. NUCLEAR MODELS

The ground-state shell-model configuration of  $\text{Br}^{82}$  indicates that it should rather definitely have negative parity, while use of Nordheim's weak coupling rule predicts a high spin. The single allowed beta group, observed in this work, to level V and the absence of other beta transitions is consistent with this interpretation.

The energy of the first excited state of  $\text{Kr}^{82}$  fits into the pattern set by the other-even nuclei surveyed by Goldhaber.<sup>20</sup> The ratio of the energy of level II to that of level I (1.92), the relative intensities of the 1.47- and 0.69-Mev transitions, and the value of the internal conversion coefficient of the 0.69-Mev radiation, which appears to be predominately  $E2$ , are all in agreement with the survey of Scharff-Goldhaber and Weneser.<sup>21</sup> Their theoretical work shows that a splitting of the threefold degenerate second vibrational level is expected as a result of coupling to the outer nucleons. It appears probable that levels I and II are vibrational in nature. One may conjecture that level III does have spin 4 and is one of the predicted second vibrational levels. The third part of the predicted triplet, with spin zero, would not be observed in this case, as it would not be excited. The energy of level IV is such that it could be the third vibrational level, which is fivefold degenerate with spins of 0, 2, 3, 4, and 6, all with positive parity. The facts that both radiations from this level

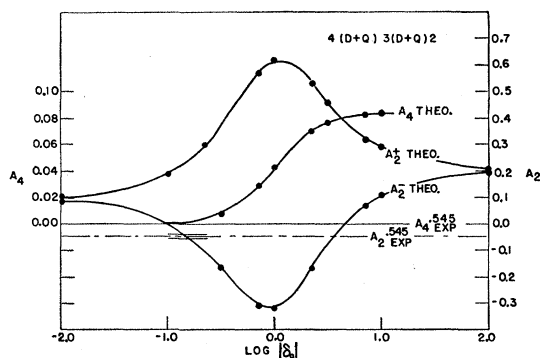


FIG. 16. Coefficients  $A_2^+$  and  $A_2^-$ , for  $\delta > 0$  and  $\delta < 0$ , respectively, and  $A_4$  as a function of  $\log|\delta|$ . Experimental values are as designated.

<sup>19</sup> Nuclear Level Schemes,  $A=40$ – $A=92$ , compiled by Way, King, McGinnis, and van Lieshout, Atomic Energy Commission Report TID-5300 (1955), p. 144.

<sup>20</sup> G. Scharff-Goldhaber, Phys. Rev. **90**, 587 (1953).

<sup>21</sup> G. Scharff-Goldhaber and J. Weneser, Phys. Rev. **98**, 212 (1955).

<sup>17</sup> M. E. Rose, Phys. Rev. **93**, 477 (1954).

<sup>18</sup> M. E. Rose, Oak Ridge National Laboratory Report ORNL-1555, 1953 (unpublished).

are predominantly  $E2$  and that the lower energy transition is more intense than the high, are both predicted by this interpretation.

Level V could be a single particle excitation of the ground state configuration.

As the ground-state configuration of  $\text{Kr}^{82}$  is subject to so many possible couplings to form excited states, many shell-model interpretations may be given.

## VI. ACKNOWLEDGMENTS

It is a pleasure to express appreciation to Dr. B. C. Carlson for helpful discussions and suggestions concerning both the theoretical and experimental aspects of the problem, to the suggestions of Dr. L. Willets concerning the nature of vibrational levels, and to Dr. Hans Frauenfelder for his advice regarding the design of the directional correlation equipment.

PHYSICAL REVIEW

VOLUME 102, NUMBER 3

MAY 1, 1956

## Neutron Cross Section of Xenon-135 as a Function of Energy

S. BERNSTEIN, M. M. SHAPIRO,\* C. P. STANFORD,† T. E. STEPHENSON,‡ AND J. B. DIAL, *Physics Department, Oak Ridge National Laboratory, Oak Ridge, Tennessee*

AND

S. FREED,§ G. W. PARKER, A. R. BROSI, G. M. HEBERT,\* AND T. W. DEWITT,|| *Chemistry Department, Oak Ridge National Laboratory, Oak Ridge, Tennessee*

(Received June 27, 1955; revised manuscript received January 26, 1956)

The neutron cross section of  $\text{Xe}^{135}$  as a function of energy was measured, using as velocity selector a focusing-type single-crystal spectrometer designed for transmission measurements of very small samples. The total cross section in the energy interval from 0.015 ev to 0.20 ev was measured. The samples, produced from neutron irradiated uranium metal, were in the form of  $\text{PdI}_2$  and were contained in sealed Pyrex capillary tubing. The largest initial strength of the samples was 10 curies of  $\text{I}^{135}$  activity, corresponding to  $12 \times 10^{15}$  atoms of  $\text{I}^{135}$ . The daughter  $\text{Xe}^{135}$  grew from the  $\text{I}^{135}$  as a known function of time, reaching a maximum value of about  $5 \times 10^{15}$  atoms of  $\text{Xe}^{135}$  11.3 hours after the  $\text{I}^{135}$  begins to decay. In the absolute assay of sample strengths, absolute  $\beta$  counting of pure  $\text{I}^{135}$  samples, and  $\beta$ - $\gamma$  coincidence counting of pure  $\text{Xe}^{135}$  samples served as primary standards. Hard gamma rays from  $\text{I}^{135}$  served as a secondary standard. The total cross section of one entire sample of Xe was of the order of 1.5 square millimeters. The transmission of the sample was measured during the period of growth and decay of the Xe. The radioactive

sample was placed inside the shield of the ORNL graphite reactor. A thermal beam of neutrons from the reactor was allowed to pass longitudinally through the sample along the axis of the capillary tube onto the quartz crystal spectrometer. The desired energies were selected by use of the Bragg reflection law,  $\lambda = 2d \sin \theta$ . A resonance in the cross section of  $\text{Xe}^{135}$  was discovered at 0.085 ev. The total cross section measurements were fitted to the single-level Breit-Wigner formula equally well with the following two sets of parameters:  $g = \frac{3}{2}$ ,  $E_0 = 0.0851 \pm 0.0011$  ev,  $\Gamma_n^0 = 0.0305 \pm 0.0008$  ev,  $\Gamma_\gamma = 0.0828 \pm 0.0031$  ev;  $g = \frac{5}{2}$ ,  $E_0 = 0.0849 \pm 0.0010$  ev,  $\Gamma_n^0 = 0.0182 \pm 0.0005$  ev,  $\Gamma_\gamma = 0.0942 \pm 0.0032$  ev.  $E_0$  is the resonance energy,  $\Gamma_n^0$  is the neutron width at resonance,  $\Gamma_\gamma$  is the gamma ray width of the level, and  $g$  is the statistical weight factor. The factor  $g$  has two possible values because the spin of the compound state is not known. The capture cross section at resonance for state with  $g = \frac{3}{2}$  is 55% of the theoretical maximum possible, and the corresponding capture cross section for the state with  $g = \frac{5}{2}$  is 80% of the theoretical maximum value.

## INTRODUCTION

THE cross section of  $\text{Xe}^{135}$  is of interest for both fundamental and applied reasons. (1) It is of interest from the point of view of nuclear structure. The cross section of  $\text{Xe}^{135}$  is the largest known neutron cross section. The value of  $\pi\lambda^2$  at the peak of the resonance, which was first characterized by this work, is approximately  $7.5 \times 10^{-18}$  cm<sup>2</sup>. The total cross section at resonance is about 0.1 of the maximum possible theoretical limit,  $4\pi\lambda^2$ . The capture cross section at resonance is about 0.4 of its maximum possible theoretical limit,  $\pi\lambda^2$ . If the spin of the target nucleus is taken into consideration, then the capture cross

section at resonance is very close, indeed, to its maximum possible theoretical limit  $g\pi\lambda^2$ , in which  $g$  is the statistical weight factor, since  $g$  for  $\text{Xe}^{135}$  probably has the value either  $\frac{3}{2}$  or  $\frac{5}{2}$ . The cross section of  $\text{Xe}^{135}$  is of interest, also, because the  $\text{Xe}^{135}$  nucleus consists of 54 protons and 81 neutrons, needing one neutron to become a magic number nucleus. (2) It is a fission product poison of such large cross section that it affects markedly the operating characteristics of chain reactors. Knowledge of the cross section of  $\text{Xe}^{135}$  as a function of energy is useful in the design of nuclear chain reactors to be operated at various temperatures.

The existence of a fission product with a very large cross section was discovered by Fermi and Wheeler in the startup of the first Hanford reactor about the end of 1944. From the dynamic behavior of the pile, they deduced that the cross section for pile neutrons was roughly  $4 \times 10^{-18}$  cm<sup>2</sup>, and was associated with a half-life of about 9 hours. This value of the half-life suggested

\* Now at Naval Research Laboratory, Washington, D. C.

† Now at Westinghouse Research Laboratories, East Pittsburgh, Pennsylvania.

‡ Now at Glenn L. Martin Aircraft Company, Baltimore, Maryland.

§ Now at Brookhaven National Laboratory, Upton, New York.

|| Now at Chemstrand Corporation, Decatur, Alabama.